

## Alpine skiing optimization: A new bio-inspired optimization algorithm

Yongliang Yuan<sup>a</sup>, Jianji Ren<sup>b,\*</sup>, Shuo Wang<sup>c</sup>, Zhenxi Wang<sup>b</sup>, Xiaokai Mu<sup>c</sup>, Wu Zhao<sup>a</sup>

<sup>a</sup> School of Mechanical and Power Engineering, Henan Polytechnic University, Jiaozuo 454003, China

<sup>b</sup> School of Software, Henan Polytechnic University, Jiaozuo 454003, China

<sup>c</sup> School of Mechanical Engineering, Dalian University of Technology, Dalian 116024, China



### ARTICLE INFO

#### Keywords:

Swarm intelligence  
Alpine skiing optimization algorithm  
Physical stamina  
Constrained optimization  
Auto drum fashioned brake

### ABSTRACT

A novel swarm intelligence optimization algorithm is proposed, which is named alpine skiing optimization (ASO). The main inspiration of the ASO originated from the behaviors of skiers competing for the championship. In the ASO, physical stamina and sprint are two essential factors for skiers to win the tournament, which are similar to the two stages of exploration and exploitation. The skiers revealed the behaviour of winning the tournament according to the static sliding and dynamic sliding. This work simulates this behaviour from a mathematical perspective and develops the ASO algorithm. The performance of the ASO algorithm is investigated, through a comparison with many competitive optimization algorithms and four constrained engineering problems. The statistical results validate that the ASO can provide competitive results compared to other state-of-the-art optimization algorithms. Furthermore, ASO is applied to optimize the parameter of an auto drum fashioned brake engineering problem. The objective function is chosen to maximize the braking efficiency coefficient. Results show that the braking efficiency factor is improved by 28.446% compared with the initial design.

### 1. Introduction

There are a variety of optimization problems, existing in engineering, science, economics, and other fields of real life, which are usually accompanied by different types of constraints [1,2]. Moreover, these problems have different characteristics, such as quadratic, cubic, nonlinear, linear. Traditional optimization techniques based on classical derivatives are insufficient in dealing with these problems [3]. To improve the ability to solve practical engineering problems, researchers have developed new optimization methods to replace the conventional approaches to solve these problems.

Various state-of-the-art optimization algorithms have been developed to solve different real-life problems, most of which are inspired by natural phenomena and the key characteristics of biological systems [3, 4]. Compared with traditional optimization algorithms, these metaheuristic optimization algorithms can provide satisfactory results for nonlinear optimization problems. In many engineering designs, generally, it is necessary to provide the best solution for highly complex constraints in a short time, which is also a great challenge. Up to now, researchers have developed several metaheuristic algorithms for solving world combinatorial or global optimization problems. For example, improved the dragonfly algorithm (IDA) [1,2,5], genetic algorithm (GA)

[6], artificial bee colony (ABC) [7], particle swarm optimization (PSO) [8], differential evolution (DE) [9], cuckoo search (CS) [10], gravitational search algorithm (GSA) [11], ant colony optimization (ACO) [12], central force optimization (CFO) [13], teaching learning based optimization (TLBO) [14], fuzzy particle swarm reinforcement learning (FPSRL) [15], hybrid swarm algorithm (HSA) [16], experiment-based approach to teach optimization techniques (OT) [17], particle swarm optimization policy (PSO-P) [18], model-free adaptive control takagi-sugeno fuzzy algorithm (CFDL-PDTSPA) [19], slime mould algorithm (SMA) [20], instinctive reaction strategy based on Harris hawks optimization (IRSHHO) [21], improved rider optimization algorithm (IROA) [22], equilibrium optimizer (EO) [23], slime mould algorithm (SMA) [24], elite opposition-based learning and chaotic k-best gravitational search strategy based grey wolf optimizer (EOCSGWO) algorithm [25], multi-objective equilibrium optimizer (MOEO) [26], generalized normal distribution optimizer (GNDO) [27], artificial hummingbird algorithm (AHA) [28], nonlinear based chaotic harris hawks optimization (NCHHO) [29], and bird mating optimizer (BMO) [30].

Although there are many kinds of metaheuristic algorithms, they all have one common feature: exploration and exploitation [31]. In the exploration stage, these optimization algorithms use the randomized algorithm to explore every area of the search space. Therefore, an

\* Corresponding author.

E-mail address: [renjianji@hpu.edu.cn](mailto:renjianji@hpu.edu.cn) (J. Ren).



Fig. 1. Preparation stage for ski game.

exploration behaviour with sufficient random characteristics ensures that the algorithm can effectively allocate more randomly generated solutions in the exploration process. The exploitation phase is usually carried out after the exploration phase. In the exploitation stage, the optimizer will focus on finding a better solution near the optimal solution in the feasible region, which strengthens the searchability of the local area, rather than the search of the whole landscape area. A good-performance optimizer should make a reasonable and delicate balance between exploration and exploitation. Otherwise, it will increase the possibility of falling into local optimum and immature convergence.

We have witnessed the application of inexpensive and efficient metaheuristics in practical engineering problems. Although the existing algorithms can be used to solve the optimization problem, they either have low accuracy or high computational cost. However, according to the ‘‘No

Free Lunch’’ theorem [32], no single algorithm can solve all the optimization problems [1,33]. Therefore, ‘‘No Free Lunch’’ theorem encourages researchers to develop more effective optimization algorithms.

A new natural heuristic optimization algorithm, named alpine skiing optimization (ASO), is proposed in this paper. The motivation of studying the ASO is to provide a state-of-the-art optimization algorithm. The main inspiration of the ASO comes from the skiers’ behaviour of competing for the champion in competitive competitions. Therefore, a new mathematical model and new equations are established in this paper. Then, the pseudo-code of the ASO is given based on the mathematical model. We propose a new mathematical model to describe all stages of the skier’s winning behaviour and show outstanding competitiveness in benchmark functions as well as on the engineering optimization problems.

The rest of this paper is organized as follows. The inspiration of the ASO is introduced in Section 2. Section 3 develops the principle and pseudocode of the ASO algorithm. The performance of the ASO is verified by the classic benchmark functions and real-world engineering problems in Section 4. Discussion of the results is presented in Section 5. The industrial application of the ASO in the brake engineering optimization problem in Section 6. Finally, Section 7 gives the concluding remarks and future work.

## 2. Inspiration

Skiing is becoming more and more of an exciting sport in winter. In a skiing game, many skiers are competing with each other, only one of whom reaches the destination first and becomes the winner of this



(a) Static sliding



(b) Dynamic sliding

Fig. 2. The stages of a ski race (a) Static sliding (b) Dynamic sliding.

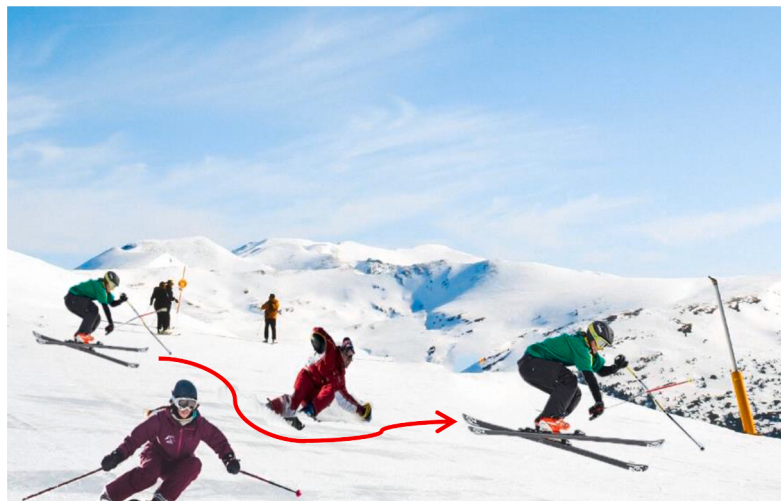


Fig. 3. The process of avoiding falling skier.

---

**Algorithm 1.** The pseudocode of the ASO.

---

**Input :** The populationsize  $N$  and maximum number of iterations  $T$

**Ouput :** Optimal solutions and the locationof skiers.

Initialize the skiers population  $X_i (i = 1, 2, \dots, n)$ ;

Initialize step vectors  $\Delta X_i (i = 1, 2, \dots, n)$ ;

**while** stopping criteria is not satisfied **do**

**for** each skier in population **do**

the distance between each skier and the first place

using Eq.(1);

calculate the physical stamina of each skier using Eq.(2).

**end for**

Find the first place of the skier;

**if** no skier fall down neighbouring anyoneskier

Update velocityvector using Eq.(3)

Update the position of the skiers using Eq.(4)

**else**

Update the position of the skiers using Eq.(5);

**else if**

Check and correct the new positionsbased on the

boundariesof variables;

**end**

**end while**

---

Fig. 4. The pseudocode of the ASO algorithm.

competition. The ultimate goal of any skier is trying their best to obtain the champion in every game. Before the game, all skiers need to stand on the same latitude and different longitude positions, as shown in Fig. 1.

During the race, skiers have two commonly used techniques: maintaining strength and sliding on the snow, as shown in Fig. 2. The former can be called static sliding (iteration phase), and the latter can be called dynamic sliding (final sprint phase). In static sliding, skiers can glide back and forth in a small area, the primary purposes are to avoid falls, and better preserve physical strength and passion for the game. In dynamic sliding, however, a large number of skiers spurt glide towards the finish line.

The main inspiration of the ASO originated from the behaviors of skiers competing for the championship. These skiing behaviors are very similar to the exploration and exploitation performance in the heuristic algorithms. The ASO algorithm is explained in detail in the following section.

### 3. Alpine skiing optimization

#### 3.1. Operators for exploration and exploitation

In the ASO, the behaviors of skiers follow some primitive principles:

- All the skiers are supposed to be independent of each other, and there is no collision between any two skiers.
- Suppose that the skiers have sufficient ability to avoid falls down caused by convex and concave terrain.
- Every skier has the capability to move randomly when someone falls down.

In the ASO, a skiing game consists of three phases, including the initialization phase, iteration phase, and final sprint phase. During the

initialization phase, each skier will obtain the current best position, then all the skiers search path to the first place. During the iteration phase, some skiers may fall down, and others must stay away from those who fall down. In the last stage, all the skiers try their best to obtain the first place. The skiing game is shown in Fig. 3.

In the initialization phase, the solution space is defined by the ASO algorithm. For the skiers, they will find their own position, which is randomly assigned at this phase. After obtaining the values of the parameters, the ASO can generate an initial population to calculate the fitness values. Notably, the total number of skiers is held a constant.

In the second phase of the ASO, namely iteration, the iterations of the ASO are performed. All the skiers move from their current positions to new positions with some regularity. Notably, the skiers will notice their ranking and move close to the first place. The fitness values of the skiers are calculated and compared with the previous results. Then the best solutions are preserved in the current iteration. The psychological change of the skiers is based on two essential issues: the first place and avoiding falling. For each skier of the ASO, the distance between each skier and the first place can be given by Eq. (1) [1]:

$$s_i(t) = \|x_i(t) - x_b(t)\| \quad (1)$$

where  $x_i(t)$  denotes the position of a skier in the iteration number  $t$ ,  $x_b(t)$  is the position of the first place the iteration number  $t$ .

During the competition, skiers will use more skiing skills to compete for the first place. As the game progresses, the physical stamina of the skiers will change accordingly, which can be defined by Eq. (2) [2,34]:

$$g_i(t) = \frac{L}{1 + e^{-k(x_i(t) - x_0)}} \quad (2)$$

where  $x_0$  denotes the  $x$ -value of the sigmoid's midpoint, which is set to 0.5;  $k$  is the logistic growth rate;  $L$  is the maximum value. The step vector

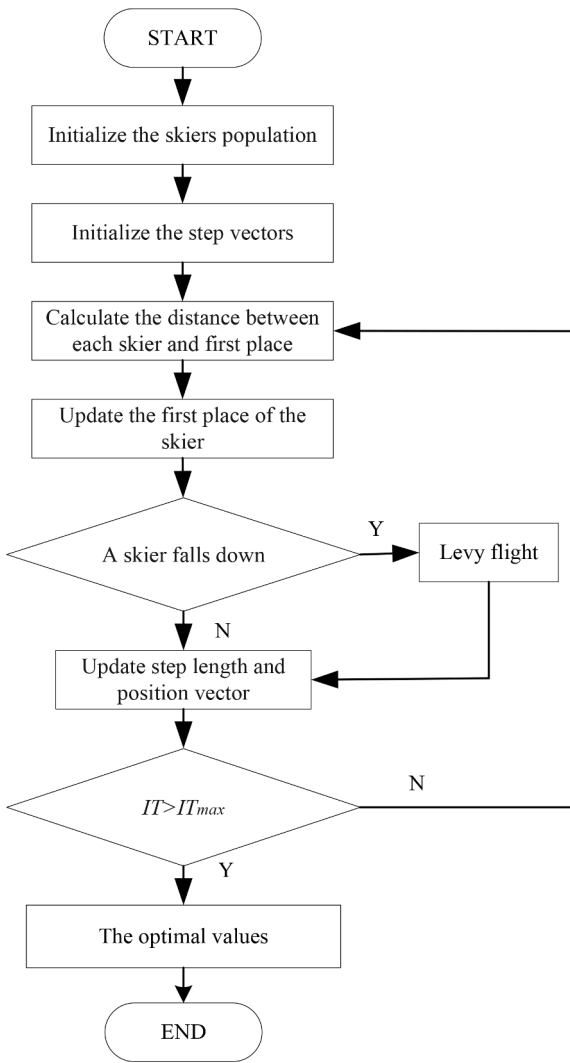


Fig. 5. The flowchart of the ASO.

**Table 1**  
Unimodal benchmark functions.

Function	Dimension	Range	$f_{\min}$
$f_1(x) = \sum_{i=1}^n x_i^2$	20,100	[-100,100]	0
$f_2(x) = \sum_{i=1}^n  x_i  + \prod_{i=1}^n  x_i $	20,100	[-100,100]	0
$f_3(x) = \sum_{i=1}^n (\sum_{j=1}^i x_j)^2$	20,100	[-100,100]	0
$f_4(x) = \max_i\{ x_i , 1 \leq i \leq n\}$	20,100	[-100,100]	0
$f_5(x) = \sum_{i=1}^{n-1} [100(x_{i+1} - x_i^2) + (x_i - 1)^2]$	20,100	[-30,30]	0
$f_6(x) = \sum_{i=1}^n ([x_i + 0.5])^2$	20,100	[-100,100]	0
$f_7(x) = \sum_{i=1}^n i x_i^4 + \text{random}(0,1)$	20,100	[-1,28,1.28]	0

and the position of the skiers can be updated using Eqs. (3) and (4), respectively.

$$\Delta \mathbf{X}(t) = r \cdot \mathbf{S}(t) \cdot \mathbf{G}(t) \quad (3)$$

$$\mathbf{X}(t+1) = \mathbf{X}(t) + \Delta \mathbf{X}(t) \quad (4)$$

where  $\mathbf{S}(s)$  and  $\mathbf{G}(g)$  are the distance matrix and physical fitness matrix of the skiers, respectively,  $r$  denotes a random number in  $(0,1)$ ,  $\mathbf{X}(t+1)$  denotes the positions of the skiers in the iteration number  $t+1$ . Some skiers may fall down during skiing because of accidents and imperfect skills.

Considering the influence of physical distance and various other

factors, such as rain, wind, and uneven slides, skiers are more likely to fall down when competing for the first place. In the ASO, "fall down" means that the skier's physical strength changes greatly relative to the previous moment's physical strength. When the difference between the two values reaches 15%, the skier is defined as a person who falls down. When the distance value is less than 0.5, the positions of other skiers are updated using a Levy flight strategy. The position of the other skiers can be calculated as follows:

$$\mathbf{X}(t+1) = \mathbf{X}(t) + \text{Levy}(\mathbf{x}(t)) \times \mathbf{X}(t) \quad (5)$$

where  $\text{Levy}(\mathbf{x})$  denotes the dimension of the skiers' positions.

The Levy flight is calculated as follows [35–37]:

$$\text{Levy}(\mathbf{x}) = 0.01 \times \frac{r_1 \times \sigma}{|r_2|^{1/\beta}} \quad (6)$$

where  $r_1$  and  $r_2$  are the random numbers in  $[0,1]$ , respectively;  $\beta$  is a constant ( $\beta = 1.5$ ), and  $\sigma$  can be obtained by:

$$\sigma = \left( \frac{\Gamma(1+\beta) \times \sin\left(\frac{\pi\beta}{2}\right)}{\Gamma(1+\beta) \times \beta \times 2^{\left(\frac{\beta-1}{2}\right)}} \right)^{\frac{1}{\beta}} \quad (7)$$

where  $\Gamma(x) = (x-1)!$ .

In the final sprint phase of the ASO, the first skier will continue along the current path. The other competitors will reconfirm the new skiing movement by combining the first place's forward direction with their current position and orientation. The iteration will stop when the convergence criterion is not matched. The stopping criterion of the ASO is set to the maximum number of iterations without improvement.

In the ASO, the search process can be divided into seven steps:

**Step 1.** Initialize the skiers' population and the step vectors.

**Step 2.** Calculate the distance between each skier and first place, we can obtain the optimal solution of the current number of iterations.

**Step 3.** Update the first place of the skiers in the current number of iterations.

**Step 4.** The ASO algorithm determines whether someone falls. When some skiers fall down, the positions of other skiers are updated using a Levy flight strategy to compete for the first place.

**Step 5.** All skiers update their position according to the first place.

**Step 6.** The algorithm identifies whether the stop search criterion is reached. When the stop criterion is reached, continue to **Step 7**; otherwise, return to **Step 2**.

**Step 7.** Output the optimal solutions.

The pseudocode and the flowchart of the ASO algorithm are shown in Figs. 4 and 5.

### 3.2. Hypotheses about the ASO algorithm

Note that the computational efficiency and the robustness of the ASO mainly depend on some factors: initialization, step vector, the distance between each skier and the first place, and updating of skiers. In the ASO, we make the following assumptions:

- It is assumed that all skiers have enough physical strength to persist until the race is finished, and have the same ability to win first place.
- Assuming that all skiers will not deliberately obstruct others, i.e., there is no malicious competition.

**Table 2**

Multimodal benchmark functions.

Function	Dimension	Range	$f_{\min}$
$f_8(x) = \sum_{i=1}^n x_i \sin(\sqrt{ x_i })$	20,100	[-500,500]	-418.9829×n
$f_9(x) = \sum_{i=1}^n [x_i^2 - 10\cos(2\pi x_i) + 10]$	20,100	[-5.12,5.12]	0
$f_{10}(x) = -20\exp\left(-0.2\sqrt{\frac{1}{n}\sum_{i=1}^n x_i^2}\right) + 20$	20,100	[-32.32]	0
$-\exp\left(\frac{1}{n}\sum_{i=1}^n \cos(2\pi x_i)\right) + c$	20,100	[-600,600]	0
$f_{11}(x) = \frac{1}{4000}\sum_{i=1}^n x_i^2 - \prod_{i=1}^n \cos\left(\frac{x_i}{\sqrt{i}}\right) + 1$	20,100	[-50,50]	0
$f_{12}(x) = \frac{\pi}{n} \times 10\sin(\pi y_1) + \frac{\pi}{n} \times (y_n - 1)^2 + \frac{\pi}{n} \sum_{i=1}^{n-1} (y_i - 1)^2 [1 + 10\sin^2(\pi y_{i+1})] + \sum_{i=1}^n u(x_i, 10, 100, 4)$	20,100	[-50,50]	0
$k(x_i - a)^m x_i > a$ $y_i = 1 + \frac{x_i + 1}{4}, u(x_i, a, k, m) = \{ 0 - a < x_i < a$ $k(-x_i - a)^m x_i < -a$	20,100	[-50,50]	0
$f_{13}(x) = 0.1\{\sin^2(3\pi x_1) + \sum_{i=1}^n (x_i - 1)^2 [1 + \sin^2(3\pi x_1 + 1)] + (x_n - 1)^2 [1 + \sin^2(3\pi x_n)]\} + \sum_{i=1}^n u(x_i, 10, 100, 4)$	20,100	[-50,50]	0

**Table 3**

Fixed-dimension multimodal benchmark functions.

Function	Dimension	Range	$f_{\min}$
$f_{14}(x) = \left(\frac{1}{500} + \sum_{j=1}^n \frac{1}{j + \sum_{i=1}^2 (x_i - a_{ij})^6}\right)^{-1}$	2	[-65,65]	1
$f_{15}(x) = \sum_{i=1}^n \left[ a_i - \frac{x_i(b_i^2 + b_i x_2)}{b_i^2 + b_i x_3 + x_4} \right]^2$	4	[-5,5]	3E-4
$f_{16}(x) = 4x_1^2 - 2.1x_1^4 + \frac{1}{3}x_1^6 + x_1 x_2 - 4x_2^2 + 4x_2^4$	2	[-5,5]	-1.032
$f_{17}(x) = \left(x_2 - \frac{5.1}{4\pi^2}x_1^2 + \frac{5}{\pi}x_1 - 6\right)^2 + 10\left(1 - \frac{1}{8\pi}\right)\cos x_1 + 10$	2	[-5,5]	3.980E-1
$f_{18}(x) = [1 + (x_1 + x_2 + 1)^2(19 - 4x_1 + 3x_1^2 - 14x_2 + 6x_1 x_2 + 3x_2^2)] \times [30 + (2x_1 - 3x_2)^2 \times (18 - 32x_1 + 12x_1^2 + 48x_2 - 36x_1 x_2 + 27x_2^2)]$	2	[-2,2]	3
$f_{19}(x) = -\sum_{i=1}^4 c_i \exp(-\sum_{j=1}^3 a_{ij}(x_j - p_{ij})^2)$	3	[1,3]	-3.86
$f_{20}(x) = -\sum_{i=1}^4 c_i \exp(-\sum_{j=1}^6 a_{ij}(x_j - p_{ij})^2)$	6	[0,1]	-3.32
$f_{21}(x) = -\sum_{i=1}^5 [(X - a_i)(X - a_i)^T + c_i]^{-1}$	4	[0,10]	-10.153
$f_{22}(x) = -\sum_{i=1}^7 [(X - a_i)(X - a_i)^T + c_i]^{-1}$	4	[0,10]	-10.403
$f_{23}(x) = -\sum_{i=1}^{10} [(X - a_i)(X - a_i)^T + c_i]^{-1}$	4	[0,10]	-10.536

**Table 4**

The parameter settings.

Algorithm	Parameter	Value
ALO	Uniform random number	[0, 1]
MFO	Convergence constant ( $\alpha$ )	[-2, -1]
	Spiral factor ( $b$ )	1
DE	Scaling factor	0.4
	Crossover probability	0.6
CMA-ES	Number of offsprings ( $u$ )	$10^*(4 + \lceil 3\ln(n) \rceil)$
	Parent weights ( $w$ )	$\frac{\log(u + 0.5) - \log(u)}{\sum_{i=1}^u w}$
	$c_{\sigma}$	$\frac{u_w + 2}{n + u_w + 5}$
	$d_{\sigma}$	$1 + 2\max\left(0, \sqrt{\frac{u_w - 1}{n + 1} - 1}\right) + \frac{u_w + 2}{n + u_w + 5}$
DA	Step length coefficient ( $\xi$ )	1
	Initial radius ( $R$ )	$(ub - lb)/10$
EOEDA	Step length coefficient ( $\xi$ )	[-1, 1]
	Initial radius ( $R$ )	$(ub - lb)/10$
ASO	Random number ( $r$ )	0.5
	Logistic growth rate ( $k$ )	0.25

- It is assumed that all skiers have enough ability to estimate the road conditions during the competition and make corresponding adjustments according to their positions.

## 4. Experimental investigation

### 4.1. Benchmark functions

The performance of the ASO is verified by 23 classic benchmark functions, which have been widely used in Refs. [38,39]. These benchmark functions have enough capacity to evaluate the performance of a novel optimization algorithm. The 23 benchmark functions are listed in Tables 1–3. It is worth noting that F1-F7 are unimodal benchmark functions, which can fully verify the convergence of the ASO algorithm. F8-F13 are multimodal functions, which are used to verify problems with multiple locally optimal solutions. The exploration ability can be tested using F14-F23. In this section, the ASO is compared with six state-of-the-art optimization algorithms, i.e., ant lion optimizer (ALO) [40], moth-flame optimization (MFO) [41], differential evolution (DE) [42], evolution strategy with covariance matrix adaptation (CMA-ES) [43], dragonfly algorithm (DA) [44], elite opposition learning and

**Table 5**

Results of unimodal benchmark functions (F1-F7), with 20 dimensions.

Functions		ALO	MFO	DE	CMA-ES	DA	EOEDA	ASO
F1	Mean	6.425E-6	6.090E-7	6.407E-3	3.439E-9	2.981E0	1.042E-19	5.415E-23
	SD	8.709E-8	5.163E-7	1.319E-4	1.465E-10	1.490E0	3.280E-20	2.450E-24
	P-value	7.888E-2	5.545E-2	7.923E-9	1.734E-13	1.425E-5	3.431E-9	2.350E-9
F2	Mean	9.979E-2	2.841E-5	1.321E-1	7.650E-5	1.331E1	1.911E-10	8.374E-9
	SD	1.483E0	1.679E-5	2.081E-2	1.938E-6	6.833E-1	6.003E-11	3.231E-10
	P-value	4.788E-4	1.507E-4	9.220E-9	1.739E-19	3.194E-6	3.405E-10	1.667E-10
F3	Mean	1.579E-2	1.274E0	1.464E2	1.027E-2	4.735E1	4.027E-24	2.708E-28
	SD	3.880E-1	1.735E1	21.923	2.190E-3	3.559E0	6.401E-24	1.440E-29
	P-value	2.829E-5	6.405E-6	6.501E-9	1.642E-2	6.438E-5	7.884E-4	3.143E-9
F4	Mean	5.001E-3	3.671E-1	1.887	3.992E-4	2.008E0	2.774E-8	1.065E-10
	SD	8.709E-3	1.279E1	2.004E-1	9.131E-5	7.871E-1	7.725E-9	2.267E-11
	P-value	6.797E-6	6.533E-6	1.189E-12	1.155E-20	7.993E-13	2.876E-5	1.968E-11
F5	Mean	2.363E2	2.745E2	3.689E2	5.278E1	3.744E4	1.917E1	1.890E1
	SD	4.775E1	7.834E1	1.338E1	2.289E1	5.527E2	2.199E-2	4.878E-2
	P-value	1.769E-1	3.998E-4	1.105E-5	2.180E-1	2.908E-3	6.050E-8	7.456E-17
F6	Mean	1.490E-6	7.729E-7	6.403E-3	3.893E-9	5.192E0	3.205E0	3.590E0
	SD	6.171E-7	2.090E-8	1.711E-4	1.877E-10	4.060E-1	4.963E-1	6.133E-1
	P-value	3.099E-2	8.011E-4	7.040E-7	3.439E-12	1.122E-3	7.743E-9	3.171E-14
F7	Mean	1.193E-2	7.509E-3	6.678E-2	4.400E-3	1.814E-1	2.305E-3	1.120E-2
	SD	1.219E-2	3.204E-3	1.416E-2	1.609E-4	1.555E-2	1.907E-4	9.615E-4
	P-value	1.755E-5	3.120E-5	1.138E-7	3.147E-15	5.033E-8	3.509E-4	1.196E-6

**Table 6**

Results of multimodal benchmark functions (F8-F13), with 20 dimensions.

Functions		ALO	MFO	DE	CMA-ES	DA	EOEDA	ASO
F8	Mean	-1.610E4	-3.861E4	-4.122E4	-1.408E4	-4.091E4	2.940E4	-1.254E4
	SD	3.145E2	2.505E2	2.988E2	3.080E2	6.630E2	3.421E2	1.592E2
	P-value	1.077E-14	1.188E-12	6.310E-11	2.382E-11	1.254E-10	2.422E-10	3.420E-13
F9	Mean	4.546E1	7.209E1	5.405E1	8.977E1	9.441E1	2.841E-13	0.000
	SD	2.659E0	2.341E1	4.971E0	9.106E0	3.953E0	8.987E-15	0.000
	P-value	7.051E-6	4.365E-6	7.290E-11	2.791E-30	2.638E-13	3.439E-1	NaN
F10	Mean	2.913E0	8.116E-1	3.851E-2	2.113E-5	2.895E0	6.662E-11	2.505E-10
	SD	4.655E-1	7.738E-2	4.803E-3	5.345E-6	7.069E-1	1.030E-12	1.143E-11
	P-value	1.217E-11	9.016E-3	1.084E-9	1.897E-19	3.827E-16	7.025E-2	3.305E-1
F11	Mean	7.722E-2	5.288E-1	9.709E-2	2.390E-8	9.811E-1	0.000	0.000
	SD	8.771E-2	2.872E-1	2.017E-2	1.291E-9	1.305E-1	0.000	0.000
	P-value	2.136E-2	2.535E-4	9.592E-8	5.235E-11	8.604E-10	NaN	6.845E-9
F12	Mean	4.728E-1	5.763E-1	4.951E-4	2.556E-10	1.504E0	4.648E-1	3.804E-2
	SD	2.967E-1	4.777E-3	1.655E-7	1.538E-12	1.833E-1	2.051E-2	2.225E-3
	P-value	7.020E-4	4.107E-4	5.584E-6	4.540E-10	1.902E-4	5.362E-5	2.929E-10
F13	Mean	6.083E-5	4.775E-1	3.710E-3	2.001E-9	3.021E0	1.810E0	1.727E0
	SD	6.793E-6	4.164E-2	1.305E-4	1.172E-9	3.090E-2	2.173E-1	3.183E-1
	P-value	4.645E-2	5.501E-3	6.923E-6	2.793E-10	3.213E-1	7.864E-10	3.054E-13

exponential function steps-based dragonfly algorithm (EOEDA) [45], which are widely used in practical optimization problems in recent five years. In the ASO, the objective function, dimensions of design variables, constraint conditions, logistic growth rate, random walk length, initialized the skiers' population, and initialized the step vectors are the parameters. The objective function, dimensions of design variables and constraint conditions need to be determined by the user. The logistic growth rate is set to 0.5. The other parameters of the ASO can be set as random. The parameters of these optimization algorithms are listed in Table 4.

To verify the accuracy and reliability of the ASO algorithm, the optimal solutions of the 23 benchmark functions of different advanced optimization algorithms were compared. The optimal solutions of the 23 benchmark functions are listed in Tables 5–7. Notably, the mean values and standard deviation (SD) data are obtained based on 50 independent optimization calculations.

Table 5 reports the competitive results of the ASO on the seven unimodal benchmark functions. Obviously, the comprehensive performance of the ASO is the best, especially in F1, F3, F4 and F5, the optimal solution can be obtained. Specifically, the ASO can obtain the optimal global solution on other unimodal functions except for F2, F6, and F7. For the p-value in Table 5, the results of the ASO are better than that of ALO, MFO, DE, CMA-ES, DA, and EOEDA. Note that the SD result of the

ASO is relatively small and has significant statistical significance. Notably, the convergence progress of F1 and F3 is given in Fig. 6. Amongst these seven optimization algorithms, the ASO has the highest convergence accuracy.

Table 6 reports the results of the multimodal functions (F8-F13). Obviously, the ASO can achieve the optimal solutions amongst the seven algorithms. For example, the ASO provides competitive results on F19-F11. From Fig. 7, the convergence speed of the ASO is faster than other state-of-the-art algorithms. From the p-values in Table 6, it can be observed that the significant advantages of the ASO are shown in most cases.

The results of fixed-dimension multimodal benchmark functions are listed in Table 7. Obviously, the ASO can provide more competitive results than other optimization algorithms. The main reason is that the ASO has superior exploration and exploitation ability, which can effectively obtain the optimal solutions. The convergence performance of F14 and F17 are plotted in Fig. 8, from which it is clear that the convergence of the ASO is faster than that of the other state-of-the-art algorithms.

To verify the influence of the ASO on different dimensions, the ASO is carried out to tackle the scalability analysis by increasing the number of dimensions. For this purpose, the results of the unimodal and multimodal benchmark functions were compared with the other state-of-the-

**Table 7**

Results of fixed-dimension multimodal benchmark functions (F14-F23).

Functions	ALO	MFO	DE	CMA-ES	DA	EOEDA	ASO
F14	Mean	6.912E0	6.934E0	6.921E0	3.688E0	7.020E0	9.971E0
	SD	0.000	0.000	9.710E-6	2.240E-1	3.041E-1	2.443E0
	P-value	NaN	1.012E-9	3.895E-8	7.131E-10	1.573E-9	4.115E-7
F15	Mean	1.730E-4	8.701E-4	7.150E-4	1.903E-3	9.102E-3	2.102E-3
	SD	1.101E-3	2.343E-4	8.831E-5	9.034E-4	8.401E-4	1.903E-4
	P-value	8.392E-4	9.104E-7	8.996E-10	2.220E-12	2.915E-4	8.204E-3
F16	Mean	-1.032E0	-1.032E0	-1.032E0	-1.032E0	-1.032E0	-1.032E0
	SD	1.776E-13	0.002	1.050E-6	6.771E-16	4.621E-4	4.990E-5
	P-value	2.061E-16	NaN	3.941E-14	1.283E-13	0.000	2.371E-14
F17	Mean	3.980E-1	3.980E-1	3.980E-1	3.980E-1	3.980E-1	3.980E-1
	SD	4.122E-13	0.000	5.715E-4	5.912E-8	4.273E-6	1.201E-3
	P-value	2.213E-19	1.085E-7	0.000	1.398E-12	7.812E-9	3.942E-12
F18	Mean	3.000E0	3.000E0	3.000E0	3.000E0	3.000E0	3.000E0
	SD	7.628E-2	1.201E-15	9.362E-16	1.454E-15	6.140E-1	7.973E-1
	P-value	6.409E-2	4.304E-14	3.315E-16	9.155E-13	0.000	4.810E-2
F19	Mean	-3.826E0	-3.862E0	-3.867E0	-3.863E0	-3.835E0	-3.822E0
	SD	5.860E-11	9.012E-16	3.903E-14	2.714E-15	1.641E-2	5.743E-2
	P-value	6.812E19	3.270E-14	4.642E-14	NaN	9.110E-10	6.367E-10
F20	Mean	-3.267E0	-3.232E0	-3.342E0	-3.270E0	-3.221E0	-3.063E0
	SD	6.314E-2	5.015E-2	1.810E-5	5.991E-2	1.665E-1	1.134E-1
	P-value	5.875E-17	8.485E-18	6.683E-9	3.783E-12	9.380E-14	2.141E-14
F21	Mean	-7.130E0	-8.125E0	-9.920E0	-9.075E0	-9.653E0	-7.880E0
	SD	3.313E0	3.290E0	4.515E-1	2.544E0	1.591E-1	1.823E0
	P-value	7.764E-5	2.663E-5	1.359E-13	2.892E-18	5.105E-15	2.535E-7
F22	Mean	-6.970E0	-8.547E0	-8.883E0	-9.891E0	-9.878E0	-8.121E0
	SD	3.636E0	3.034E0	1.486E0	1.940E-1	1.673E-1	1.194E-1
	P-value	1.871E-4	9.273E-6	1.942E-14	1.570E-22	1.314E-10	4.825E-9
F23	Mean	-5.694E0	-9.180E0	-10.421E0	-10.514E0	-8.369E0	-7.96E0
	SD	3.490E0	2.921E0	2.590E-1	1.813E-2	2.770E-1	2.087E0
	P-value	6.021E-4	3.743E-6	5.831E-10	1.585E-9	5.563E-13	7.791E-7

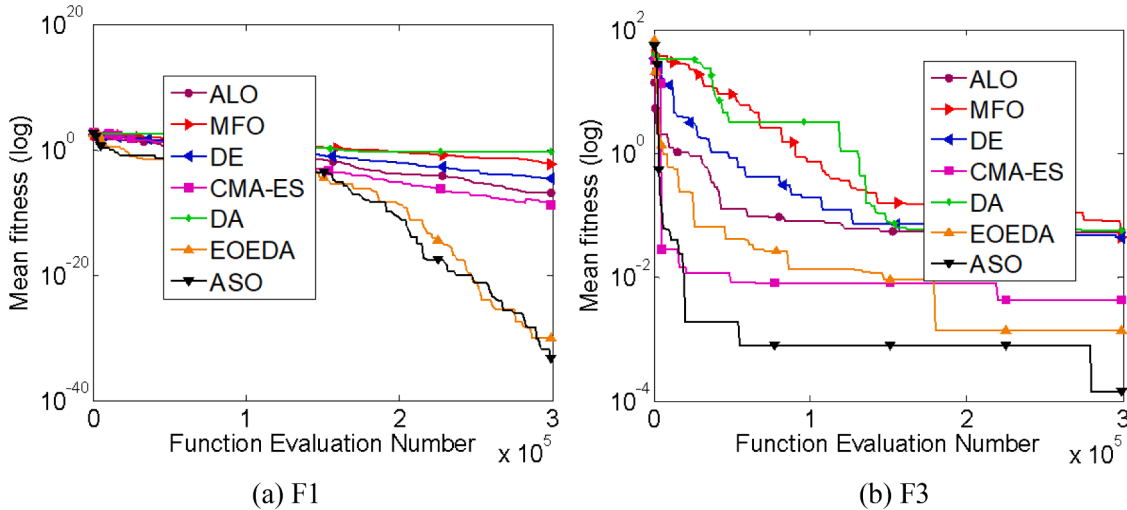


Fig. 6. Convergence of the F1 and F3.

art optimization algorithms with 100 dimensions. All the optimization algorithms were performed independently for 50 runs. Table 8 provides the mean values and standard deviation (SD) of the unimodal and multimodal benchmark functions.

The results of the benchmark functions with 100 dimensions are listed in Table 8. Notably, the ASO can provide very competitive results, and can be capable of obtaining the optimal solutions and outperforming the other popular algorithms. The second-best results belong to the CMA-ES, followed by EOEDA, ALO, DE, DA, and MFO. According to p-values in Table 9, it is shown that the solutions of ASO are better than those of the other optimization algorithms in most cases. In view of the above-mentioned results, we conclude that the ASO can be used as an efficient algorithm to solve engineering problems.

#### 4.2. Constrained engineering optimization problems using the ASO

This section will discuss the performance of the ASO in solving constrained engineering problems. Four benchmark engineering problems, i.e., three-bar truss design, multiple disc clutch brake, speed reducer, and rolling element bearing design are selected for performance evaluation of the ASO. These four benchmark engineering problems are composed of several equality constraints and inequality constraints, which can fully evaluate the performance of the ASO from the perspective of the ability to handle constraints.

##### 4.2.1. Three-bar truss design

The three-bar truss (see Fig. 9) design optimization problem has been widely studied in previous works [46]. This optimal design model

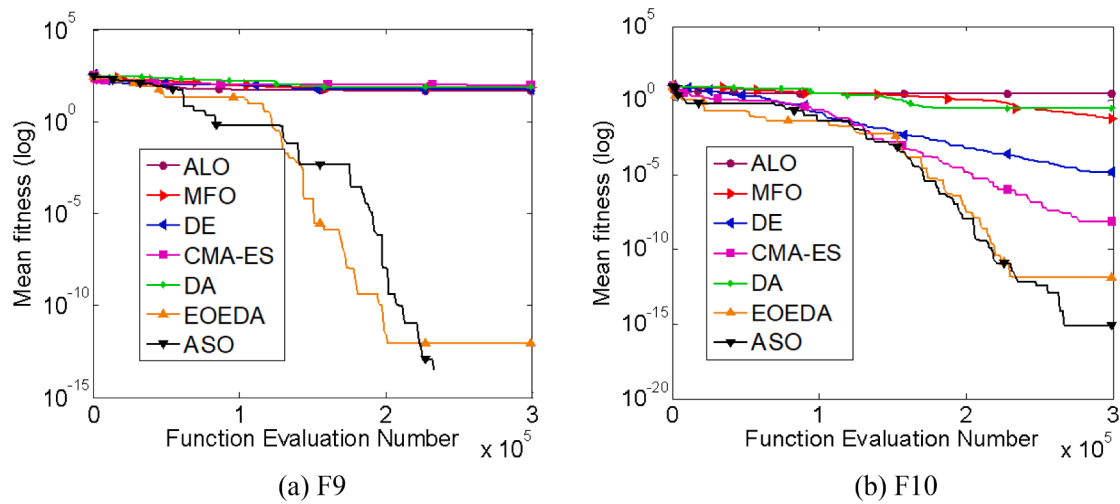


**Fig. 7.** Convergence of the F9 and F10.

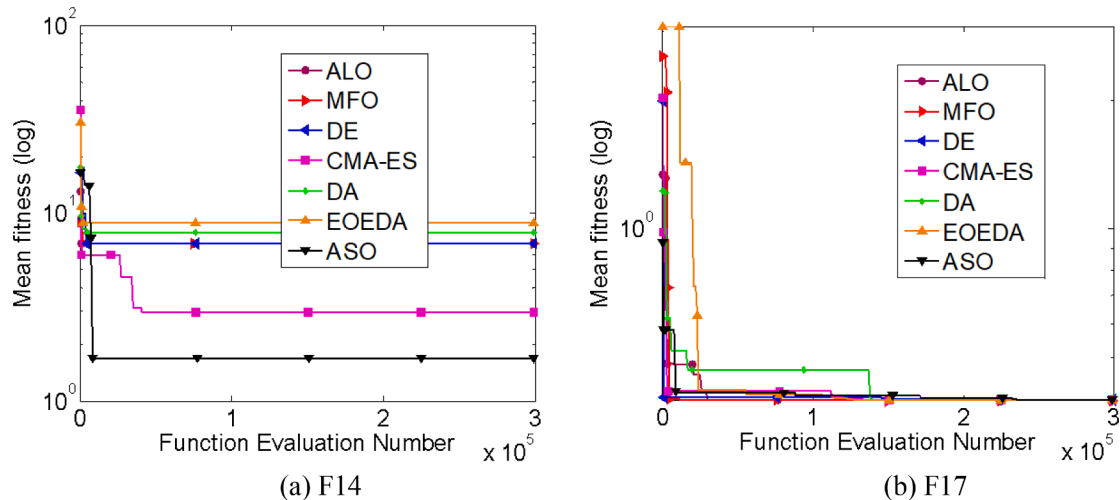


**Fig. 8.** Convergence of the F14 and F17.

consists of two design variables and three inequality constraints, which can be described as follows:

$$\begin{aligned}
 & \text{consider } \mathbf{X} = [x_1, x_2] = [A_1, A_2] \\
 & \min f(\mathbf{X}) = \left(2\sqrt{2}x_1 + x_2\right) \times l \\
 & \text{s.t. } g_1(\mathbf{X}) = \frac{\sqrt{2}x_1 + x_2}{\sqrt{2x_1^2 + 2x_1x_2}} p - \sigma \leq 0 \\
 & g_2(\mathbf{X}) = \frac{x_2}{\sqrt{2x_1^2 + 2x_1x_2}} p - \sigma \leq 0 \\
 & g_3(\mathbf{X}) = \frac{\sqrt{2}x_1 + x_2}{\sqrt{2x_2^2 + x_1}} p - \sigma \leq 0 \\
 & 0 \leq x_1, x_2 \leq 1, \quad l = 100\text{cm} \\
 & p = 2\text{KN/cm}^2, \quad \sigma = 2\text{KN/cm}^2
 \end{aligned} \tag{8}$$

Table 10 reports the results of the three-bar truss design case. The results of the ASO are compared with those of the five optimization algorithms, i.e., MFO [41], CS [47], Tsa [48], Ray and Sain [49], PSO-DE [50], and AHA [51] in previous literature. To verify the performance of the ASO algorithm, the results of the ASO were compared with the results of the five optimization algorithms. Interestingly, the ASO can reveal very competitive results, it can be concluded that the ASO can efficiently handle constrained engineering problems.

#### *4.2.2. Multiple disc clutch brake*

The objective of the benchmark engineering problem is to minimize the weight of the multiple disc clutch brake as shown in Fig. 10. The design variables are the thickness of discs, the number of friction surfaces, actuating force, inner radius, and outer radius [22]. This benchmark engineering problem can be formulated as follows:

$$\begin{aligned}
& \text{consider } \mathbf{X} = [x_1, x_2, x_3, x_4, x_5] = [t, r_i, r_0, F, Z] \\
& \min f(\mathbf{X}) = \pi t (r_0^2 - r_i^2) (Z + 1) \rho \\
& \text{s.t. } g_1(\mathbf{X}) = r_o - r_i - \Delta r \geq 0 \\
& g_2(\mathbf{X}) = l_{\max} - (Z + 1)(t + \delta) \geq 0 \\
& g_3(\mathbf{X}) = p_{\max} - p_{rz} \geq 0 \\
& g_4(\mathbf{X}) = p_{\max} v_{sr\max} - p_{rz} v_{sr} \geq 0 \\
& g_5(\mathbf{X}) = v_{sr\max} - v_{sr} \geq 0 \\
& g_6(\mathbf{X}) = T_{\max} - T \geq 0 \\
& g_7(\mathbf{X}) = M_h - sM_s \geq 0 \\
& g_8(\mathbf{X}) = T \geq 0 \geq 0
\end{aligned} \tag{9}$$

where

$$\begin{aligned}
M_h &= \frac{2}{3} \mu F Z \frac{r_o^3 - r_i^3}{r_o^2 - r_i^2}, P_{rz} = \frac{F}{\pi(r_o^2 - r_i^2)} \\
v_{sr} &= \frac{2\pi n(r_o^3 - r_i^3)}{90(r_o^2 - r_i^2)}, T = \frac{l_z \pi n}{30(M_h + M_f)} \\
\Delta r &= 20mm, 1.5mm \leq t \leq 3mm, l_{\max} = 30mm \\
Z_{\max} &= 10, v_{sr\max} = 10m/s, \mu = 0.5, s = 1.5 \\
M_s &= 40Nm, M_f = 3Nm, n = 250rpm, \\
P_{\max} &= 1MPa, I_z = 55kg\cdot mm^2, \\
T_{\max} &= 15s, F_{\max} = 1000N, \\
r_{\min} &= 55mm, r_{\max} = 110mm
\end{aligned}$$

The optimum solutions of the ASO versus those attained by WCA [52], TLBO [53], PVS [54], HHO[3], and ABC [55] algorithms are listed in Table 11. From Table 11, we can summarize that the ASO and HHO have the same competitiveness, and the performance of WCA, TLBO, and PVS is similar. The results show that the ASO can find the best parameter combination of multiple disc clutch brake.

#### 4.2.3. Speed reducer design problem

This engineering problem is the speed reducer optimization design, which is shown in Fig. 11. The purpose of the benchmark engineering problem is to minimize the weight. In this case, there are seven design variables (i.e., the length of the first shaft between bearings, the length of the second shaft between bearings, the number of teeth in the pinion, module of the teeth, the diameter of the first shaft and second shaft, face wide, and the number of teeth in the pinion) and eleven constraints. The optimization model can be given by:

**Table 12** reports the results of the speed reducer problem. The performance of the ASO is compared with that of HEAA [56], PSO-DE [57], DELC [58], IRSHHO [21], and MVDE [59], which have been studied in the previous literature [56–59]. By comparing the results of different optimization algorithms in Table 12, it can be seen that the ASO has superior competitiveness.

#### 4.2.4. Rolling element bearing design problem

The overall configuration of the rolling element bearing design problem is shown in Fig. 12. The purpose of this case is to maximize the dynamic load-carrying capacity. This case consists of 10 design variables and nine constraints. The formulation of the rolling element bearing design problem can be formulated as follows:

$$\begin{aligned}
\text{maximize } C_d &= f_c Z^{2/3} D_b^{1.8} \text{ if } D \leq 25.4mm \\
C_d &= 3.647 f_c Z^{2/3} D_b^{1.4} \text{ if } D > 25.4mm \\
\text{s.t. } g_1 &= \frac{\varphi_0}{2\sin^{-1}(D_b/D_m)} - Z + 1 \leq 0 \\
g_2 &= 2D_b - K_{D\min}(D - d) > 0 \\
g_3 &= K_{D\max}(D - d) - 2D_b \geq 0 \\
g_4 &= \zeta B_w - D_b \leq 0 \\
g_5 &= D_m - 0.5(D + d) \geq 0 \\
g_6 &= (0.5 + e)(D + d) - D_m \geq 0 \\
g_7 &= 0.5(D - D_m - D_b) - \varepsilon D_b \geq 0 \\
g_8 &= f_i \geq 0.515 \\
g_9 &= f_0 \geq 0.515
\end{aligned} \tag{11}$$

$$\begin{aligned}
\min f(\mathbf{X}) &= 0.7854x_1x_2^2(3.3333x_3^2 + 14.9334x_3 - 43.0934) - 1.508x_1(x_6^2 + x_7^2) + 7.4777(x_6^3 + x_7^3) \\
\text{s.t. } g_1(\mathbf{X}) &= \frac{27}{x_1x_2^2x_3} - 1 \leq 0 \\
g_2(\mathbf{X}) &= \frac{397.5}{x_1x_2^2x_3^2} - 1 \leq 0 \\
g_3(\mathbf{X}) &= \frac{1.93x_4^3}{x_2x_3x_6^4} - 1 \leq 0 \\
g_4(\mathbf{X}) &= \frac{1.93x_5^3}{x_2x_3x_7^4} - 1 \leq 0 \\
g_5(\mathbf{X}) &= \frac{\sqrt{((745x_4/(x_2x_3))^2 + 16.9 \times 10^6)}}{110.0x_6^3} - 1 \leq 0 \\
g_6(\mathbf{X}) &= \frac{\sqrt{((745x_4/(x_2x_3))^2 + 157.5 \times 10^6)}}{85.0x_7^3} - 1 \leq 0 \\
g_7(\mathbf{X}) &= \frac{x_2x_3}{40} - 1 \leq 0 \\
g_8(\mathbf{X}) &= \frac{5x_2}{x_1} - 1 \leq 0 \\
g_9(\mathbf{X}) &= \frac{x_1}{12x_2} - 1 \leq 0 \\
g_{10}(\mathbf{X}) &= \frac{1.5x_6 + 1.9}{x_4} - 1 \leq 0 \\
g_{11}(\mathbf{X}) &= \frac{1.1x_7 + 1.9}{x_5} - 1 \leq 0 \\
2.6 \leq x_1 &\leq 3.6, 0.7 \leq x_2 \leq 0.8, 17 \leq x_3 \leq 28, 7.3 \leq x_4 \leq 8.3 \\
7.8 \leq x_5 &\leq 8.3, 2.9 \leq x_6 \leq 3.9, 5.0 \leq x_7 \leq 5.5
\end{aligned} \tag{10}$$

**Table 8**

Results of unimodal and multimodal benchmark functions (F1-F13), with 100 dimensions.

Functions	ALO	MFO	DE	CMA-ES	EOEDA	DA	ASO	
F1	Mean	1.856E4	1.232E5	3.409E4	8.940E1	1.291E4	1.942E4	2.991E2
	SD	5.655E3	1.329E4	2.572E3	1.022E1	7.810E3	1.146E4	8.820E1
F2	Mean	2.997E2	3.525E2	1.891E2	1.685E1	1.122E2	1.185E2	9.571E1
	SD	9.451E1	2.551E1	9.590E0	1.763E0	5.505E1	4.550E1	2.125E0
F3	Mean	6.875E4	3.030E5	4.711E5	1.950E5	1.679E5	2.615E5	2.103E2
	SD	1.270E4	7.312E4	6.173E4	5.592E4	6.171E4	8.969E4	6.460E0
F4	Mean	3.321E1	9.121E1	9.165E1	9.620E0	4.428E1	6.061E1	7.828E0
	SD	5.763E0	1.526E0	6.004E-1	8.725E-1	9.374E0	6.453E0	6.559E-1
F5	Mean	5.760E6	3.998E8	8.201E7	5.226E3	1.631E7	1.325E7	9.791E1
	SD	2.388E5	1.231E8	1.472E7	2.898E3	6.682E6	6.622E6	4.640E-2
F6	Mean	2.104E4	1.156E5	3.513E4	9.860E1	1.923E4	2.924E4	2.345E1
	SD	5.956E3	1.807E4	2.875E3	1.684E1	1.149E4	8.198E3	5.120E-1
F7	Mean	1.288E1	5.295E2	1.078E2	3.601E-2	2.101E1	9.541E2	1.620E-3
	SD	4.879E0	8.472E1	1.491E1	1.324E-2	1.542E0	2.072E2	1.130E-3
F8	Mean	-3.541E5	-3.385E5	-2.509E5	-6.563E5	-1.480E6	-2.663E6	-4.990E5
	SD	4.795E2	5.115E3	6.012E3	9.735E2	1.992E2	7.848E2	3.151E2
F9	Mean	4.580E2	9.910E2	9.735E2	8.175E2	6.909E2	9.452E2	0.000
	SD	6.411E1	6.055E1	2.152E1	2.142E1	1.872E2	9.678E1	1.945E-1
F10	Mean	1.460E1	2.013E1	1.702E1	2.985E0	1.380E1	1.474E1	1.161E1
	SD	6.193E-1	7.911E-2	3.574E-1	1.814E-1	2.105E0	2.203E0	2.070E0
F11	Mean	1.824E2	1.124E3	3.246E2	1.867E0	2.181E2	2.455E2	0.000
	SD	5.433E1	1.455E2	3.605E1	1.330E-1	8.627E1	1.286E2	5.129E-4
F12	Mean	1.748E5	7.759E8	1.628E8	1.503E0	4.824E6	9.237E6	1.035E0
	SD	2.759E4	1.844E8	3.309E7	4.219E-1	7.436E5	1.142E5	8.341E-2
F13	Mean	5.067E6	1.480E9	3.270E8	2.695E1	3.822E7	4.080E7	9.890E0
	SD	2.621E6	3.435E8	4.275E7	2.978E0	2.895E7	2.912E7	2.303E-3

**Table 9**

p-values of the Wilcoxon rank-sum test for F1-F13 with 100 dimensions.

Functions	ALO	MFO	DE	CMA-ES	EOEDA	DA	ASO
F1	3.130E-6	3.190E-10	1.278E-11	8.899E-10	4.523E-4	5.570E-4	3.105E-10
F2	3.435E-1	8.621E-12	3.472E-13	2.362E-10	1.875E-5	1.201E-4	1.870E-10
F3	3.541E-8	3.615E-7	1.710E-9	1.574E-6	7.044E-6	1.241E-5	3.336E-10
F4	2.030E-8	1.558E-11	3.623E-10	6.442E-11	2.722E-10	1.185E-7	4.404E-11
F5	3.217E-5	2.913E-6	2.751E-8	2.864E-4	1.420E-4	2.984E-5	1.941E-31
F6	1.439E-5	7.912E-9	2.542E-11	1.733E-8	1.335E-6	4.656E-4	1.763E-16
F7	1.625E-5	1.018E-8	2.915E-9	1.228E-5	1.440E-7	1.910E-3	1.207E-13
F8	2.672E-14	7.319E-10	3.136E-16	5.655E-11	2.128E-6	3.458E-9	6.558E-10
F9	3.101E-9	1.824E-12	2.017E-16	9.214E-16	1.770E-10	9.606E-7	NaN
F10	7.193E-14	3.807E-12	1.278E-14	1.740E-12	5.459E-9	6.399E-9	1.101E-11
F11	2.160E-6	1.557E-9	3.952E-10	7.695E-12	1.834E-4	2.267E-5	NaN
F12	7.675E-2	3.132E-7	8.403E-8	1.278E-6	3.090E-2	7.030E-2	2.040E-11
F13	1.794E-4	2.525E-7	1.634E-9	4.246E-10	1.608E-3	2.405E-3	2.719E-13

where

$$f_c = 37.91 \left[ 1 + \left\{ 1.04 \left( \frac{1-\gamma}{1+\gamma} \right)^{1.72} \left( \frac{f_i(2f_0-1)}{f_0(2f_i-1)} \right)^{0.41} \right\}^{10/3} \right]^{-0.3}$$

$$\times \left[ \frac{\gamma^{0.3}(1-\gamma)^{1.39}}{(1+\gamma)^{1/3}} \right] \left[ \frac{2f_i}{2f_i-1} \right]^{0.41}$$

$$x = \left[ \{(D-d)/2 - 3(T/4)\}^2 + \{D/2 - T/4 - D_b\}^2 - (d/2 + T/4)^2 \right]$$

$$y = 2\{(D-d)/2 - 3(T/4)\}\{D/2 - T/4 - D_b\}$$

$$\varphi_0 = 2\Pi - \cos^{-1} \left( \frac{x}{y} \right)$$

$$\gamma = \frac{D_b}{D_m}, f_i = \frac{r_i}{D_b}, f_0 = \frac{r_0}{D_b}, T = D - d - 2D_b$$

$$D = 160, d = 90$$

$$B_w = 30, r_i = r_0 = 11.033, 0.5(D+d) \leq D_m \leq 0.6(D+d)$$

$$0.15(D-d) \leq D_b \leq 0.45(D-d), 4 \leq Z \leq 50, 0.515 \leq f_i$$

$$f_0 \leq 0.6, 0.4 \leq K_{D\min} \leq 0.5, 0.6 \leq K_{D\max} \leq 0.7$$

$$0.3 \leq \varepsilon \leq 0.4, 0.02 \leq e \leq 0.1, 0.6 \leq \zeta \leq 0.85$$

For the rolling element bearing design problem, [Table 13](#) reports the optimal results of the proposed ASO, which is compared with those of HHO [3], TLBO [53], PVS [54], GA4 [60], and MRFO [61]. By comparing the results, it can be seen from [Table 13](#) that the ASO and HHO can obtain competitive optimal solutions compared with GA4, TLBO, and PVS. Therefore, we can conclude that the ASO is the best optimizer and can obtain better results than other optimization algorithms.

## 5. Discussion on results

According to the results of the above benchmark functions and engineering problems, it can be clearly seen from [Tables 5–7](#) that the ASO algorithm has significantly superior results compared to the other optimization algorithms (such as ALO, MFO, DE, CMA-ES, DA, and EOEDA). It is worth noting that the performance of all optimization algorithms decreases as the dimension of the benchmark function increases. Comparing the results in [Tables 8](#) and [9](#), it can be seen that the scalability of the ASO and CMA-ES algorithms are significantly better than that of ALO, MFO, DE, EOEDA and DA, and the performance of CMA-ES is still lower than that of the ASO. Notably, there are significant differences in the performance of optimization algorithms, and the result also supports the necessity to develop a novel optimization

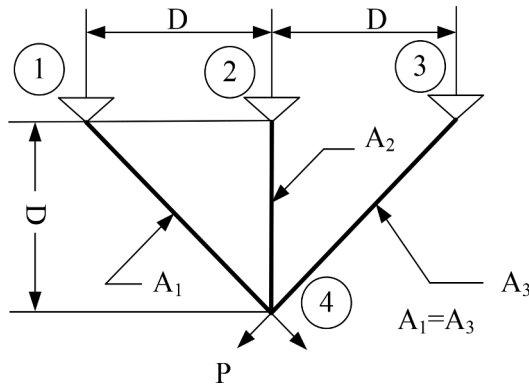


Fig. 9. The three-bar truss design.

**Table 10**  
The results of the three-bar truss design.

Algorithm	Optimum variables		Optimal solution
	$x_1$	$x_2$	
MFO [41]	0.789	0.409	263.896
CS [47]	0.789	0.409	263.972
Tsa [48]	0.788	0.408	263.680
Ray and Sain [49]	0.795	0.395	264.300
PSO-DE [50]	0.789	0.408	263.896
AHA [51]	0.789	0.408	263.896
ASO	0.789	0.408	263.896

algorithm for the ASO. Figs. 9–12 are classic engineering problems with nonlinear constraints. From Tables 10–13, it can be seen that the ASO can obtain a globally optimal solution. These results show that the ASO algorithm can obtain superior and competitive solutions in a diversified search space. Based on the above results, we can conclude that the ASO is one of the top optimizers. The ASO has a variety of exploratory and pioneering mechanisms, which can effectively avoid falling into the optimal solution when solving different types of problems.

The following features can summarize the superiority of the ASO algorithm in solving optimization problems:

- The physical stamina of the skiers changes dynamically, which can further promote the exploration and exploitation patterns of the ASO.

- The skiers determine the distance between their position and the championship position in real-time, which helps to improve the ability of global search.
- When someone slips and falls, nearby skiers use the Levy flight strategy to adjust the direction and step length, which can balance the local searchability.
- The ASO makes full use of the changing trend of skiers' physical stamina and Levy flight strategy, which can help skiers choose the best movement step.
- The time-varying parameters of the physical stamina allow the ASO to deal with the difficulty of search space and search step size, including the multi-modality and local optimal solutions.

## 6. Optimization of an auto drum fashioned brake

### 6.1. The optimization model of an auto drum fashioned brake

The safety and reliability of automobiles have become a factor of attention that affects automobile sales. It is worth noting that the drum brakes are widely used in braking systems [21]. To improve braking performance, the ASO is applied to improve the braking efficiency coefficient. Fig. 13 shows the structural parameters and forces of the auto drum fashioned brake.

In Fig. 13,  $F_1$  and  $R_1$  are the pressing force and the radius of the frictional force, respectively.  $\delta_1$  is the angle between  $x_0$  axis and the  $F_1$ . Notably, we assume that the leading shoes have the same parameters in this engineering design. In this automatic drum brake, this optimization model can be described by six design variables and four constraints:

$$\begin{aligned} \text{Consider } \vec{x} &= [x_1, x_2, x_3, x_4, x_5, x_6] = [\alpha', \beta, R, c', c, a] \\ \max f(x) &= \frac{u(x_6 + x_5)}{x_4(\cos\delta_1 + \sin\delta_1) - uR_1} + \frac{u(x_6 + x_5)}{x_4(\cos\delta_2 + \sin\delta_2) - uR_2} \\ \text{s.t. } g_1(x) &= u - \frac{x_4 \cos\delta_1}{R_1 - x_4 \sin\delta_1} \leq 0 \\ g_2(x) &= \frac{\pi d^2 p(x_6 + x_5) R_1}{b_1 x_3^2 [\cos x_1 - \cos(x_1 + \beta)] [x_4 (\cos\delta_1 + \sin\delta_1) - uR_1]} - 1.6 \leq 0 \\ g_3(x) &= \frac{x_4 x_2}{(x_6 + x_5) \sin \frac{x_2}{2}} - 2 \leq 0 \\ g_4(x) &= \frac{mv_0^2}{800 t x_1 x_2} - 1.9 \leq 0 \end{aligned} \quad (12)$$

where  $u$  is the friction factor,  $c$  and  $c'$  are the central sites of the brake shoe pin,  $t$  and  $b_1$  are braking time and the width of the brake, respectively;  $m$  and  $v_0$  denote the mass of the vehicle and the initial velocity, respectively. The angles and radius of the frictional force can be given by:

$$\delta_1 = \delta_2 = \arctan \left[ \frac{\cos 2x_1 - \cos 2(x_1 + x_2)}{2x_2 - \sin 2(x_1 + x_2) + \sin 2x_1} \right] \quad (13)$$

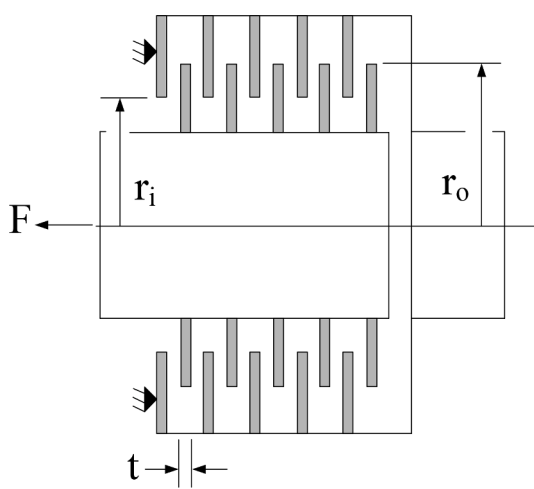
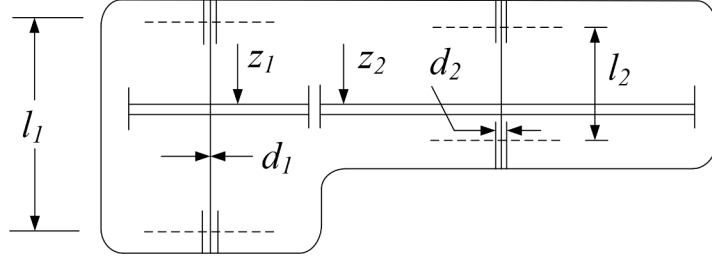


Fig. 10. Multiple disc clutch brake.

**Table 11**  
The results of multiple disc clutch brake.

Algorithm	Optimum variables					Optimal solution
	$t$	$r_i$	$r_o$	$F$	$Z$	
WCA [52]	1	70	90	910	3	0.31
TLBO [53]	1	70	90	810	3	0.31
PVS [54]	1	70	90	980	3	0.31
HHO [3]	1	70	90	1000	2.31	0.26
ABC [55]	1	71	91	849	3	0.32
ASO	1	69.99	90	990	2.98	0.26



**Fig. 11.** The speed reducer problem.

**Table 12**

Comparison of results for speed reducer problem.

Algorithm	Optimum variables							Optimal solution
	$x_1$	$x_2$	$x_3$	$x_4$	$x_5$	$x_6$	$x_7$	
HEAA [56]	3.50	0.70	17.00	7.30	7.72	3.35	5.29	2994.50
PSO-DE [57]	3.50	0.70	17.00	7.30	7.80	3.35	5.29	2996.35
DELC [58]	3.50	0.70	17.00	7.30	7.72	3.35	5.27	2994.47
IRSHHO [21]	3.56	0.70	17.00	7.50	7.80	3.67	5.29	2858.90
MVDE [59]	3.50	0.70	17.00	7.30	7.72	3.35	5.27	2994.47
ASO	5.56	0.70	17.00	7.35	7.82	3.35	5.29	2858.89

$$R_1 = R_2 = \frac{4x_3[\cos x_1 - \cos(x_1 + x_2)]}{\sqrt{[\cos 2x_1 - \cos 2(x_1 + x_2)]^2 + [2x_2 - \sin 2(x_1 + x_2) + \sin 2x_1]^2}} \quad (14)$$

## 6.2. Optimization results

The ASO algorithm is performed to solve the optimization model of the automatic drum brake. The optimization results are listed in **Table 14**. From the optimization results, it can be seen that the braking efficiency coefficient has been increased from 2.960 to 3.802, which is increased by 28.446% relative to the initial value. The convergence curve of the auto drum fashioned brake is shown in **Fig. 14**. Specifically, the ASO can obtain the optimal solution at the 183rd iteration. It clearly indicates that the ASO can quickly obtain the optimal solution of the auto drum fashioned brake.

**Table 15** reports the optimization results of these state-of-the-art optimization algorithms, including ASO, DA, MFO, HHO, CMA-ES and

ABC. From the **Table 15**, the ASO and CMA-ES algorithms can obtain the optimal solution of the auto drum fashioned brake compared with other optimization algorithms. The second-best results belong to the HHO, followed by MFO, ABC, and DA. In view of the above-mentioned results, we conclude that the ASO is an efficient optimization algorithm.

## 7. Conclusion

In this work, a novel metaheuristic optimization algorithm, namely alpine skiing optimization (ASO), is proposed to tackle the optimization problems. The ASO algorithm is inspired by the behaviors of skiers competing for the championship, which consists of three phases, i.e. initialization phase, iteration phase, and final sprint phase. In the ASO, the skier's behaviors are described by several equations. Notably, the physical fitness of each skier has been taken into account. The performance of the ASO is investigated by twenty-three unconstrained benchmark functions (i.e. unimodal benchmark functions, multimodal functions, and fixed-dimension multimodal benchmark functions) and

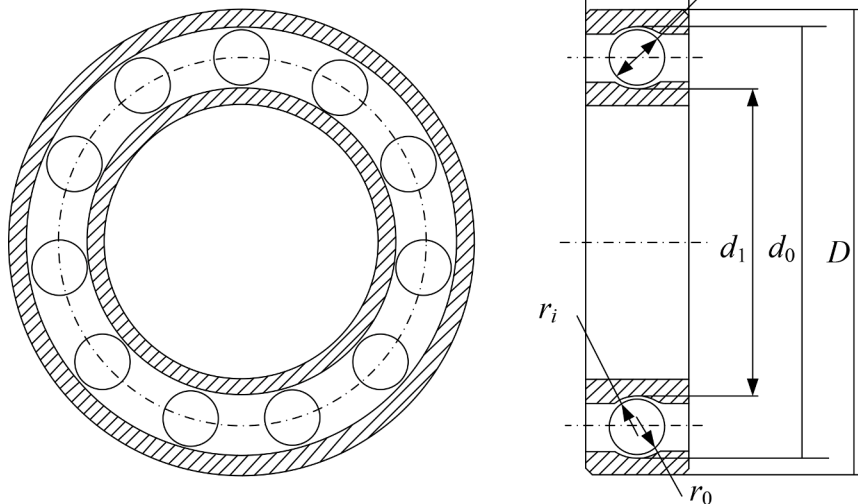


**Fig. 12.** Rolling element bearing design problem.

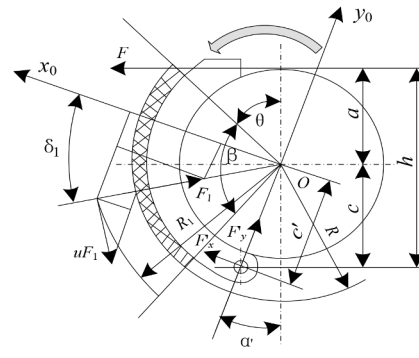
**Table 13**

Comparison of results for rolling element bearing design problem.

Algorithm	HHO [3]	TLBO [53]	PVS [54]	GA4 [60]	MRFO [61]	ASO
$D_m$	125.00	125.72	125.72	125.72	125.72	125.00
$D_b$	21.00	21.43	21.43	21.42	21.42	21.42
$z$	11.09	11.00	11.00	11.00	11.00	11.09
$f_1$	0.52	0.52	0.52	0.52	0.52	0.52
$f_0$	0.52	0.52	0.52	0.52	0.52	0.52
$K_{D\min}$	0.40	0.42	0.40	0.42	0.41	0.40
$K_{D\max}$	0.60	0.63	0.68	0.65	0.69	0.61
$\epsilon$	0.30	0.30	0.30	0.30	0.69	0.30
$e$	0.05	0.07	0.08	0.02	0.30	0.05
$\zeta$	0.60	0.80	0.70	0.75	0.05	0.60
Maximumcost	83,011.88	81,859.74	81,859.74	81,843.30	85,549.24	83,011.88



(a)



(b)

**Fig. 13.** Structural parameters and force diagram.

four constrained engineering optimization problems. The results indicate that the ASO can obtain competitive results and can be used as a state-of-the-art optimization algorithm to solve engineering optimization problems. Additionally, the results of four engineering optimization problems reveal that the ASO could provide superior solutions compared to the other well-regarded algorithms.

In addition, the ASO is applied to optimize the braking efficiency coefficient of an auto drum fashioned brake. Results show that the braking efficiency factor of the auto drum fashioned brake can be improved by 28.446% compared with the initial design. For future works, the multi-objective and binary versions of the ASO can be developed. Moreover, we can improve the ASO by considering the physical strength and resistance of skiers and quantifying the assumptions in the ASO algorithm. In particular, the ASO can be utilized to solve high-dimensional nonlinear optimization problems.

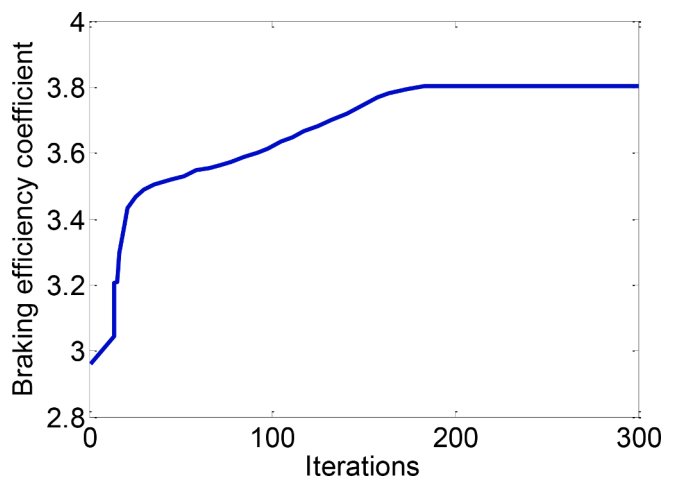
#### CRediT authorship contribution statement

**Yongliang Yuan:** Methodology, Investigation, Writing – original draft, Writing – review & editing. **Jianji Ren:** Methodology, Writing –

review & editing. **Shuo Wang:** Writing – review & editing. **Zhenxi Wang:** Validation. **Xiaokai Mu:** Methodology, Software. **Wu Zhao:** Investigation, Writing – original draft.

#### Declaration of Competing Interest

All co-authors have seen and agree with the contents of the manuscript, and there is no financial interest to report. We certify that the submission is not under review at any other publication.

**Fig. 14.** The convergence curve of the auto drum fashioned brake.

Note: “+” (“-”) denotes the increase (decrease).

**Table 14**

Optimization results of the ASO for the auto drum fashioned brake.

Design variable	Initial value (unite)	Optimal value (unite)	Improved (%)
$x_1$	25.000°	23.900°	-4.400
$x_2$	105.000°	119.600°	+13.904
$x_3$	180.000	190.000	+5.556
$x_4$	148.000	142.000	-4.0540
$x_5$	140.000	147.670	+5.479
$x_6$	140.000	149.050	+6.464
$f$	2.960	3.802	+28.446

**Table 15**

Optimization results of these state-of-the-art optimization algorithms.

Algorithm	ASO	DA	MFO	HHO	CMA-ES	ABC
$x_1$	23.900°	23.850°	23.870°	23.900°	23.900°	23.920°
$x_2$	119.600°	120.300°	119.750°	119.810°	119.600°	120.000°
$x_3$	190.000	192.200	189.200	190.030	190.000	189.900
$x_4$	142.000	143.500	142.800	141.900	142.000	141.950
$x_5$	147.670	147.910	147.050	148.000	147.670	148.730
$x_6$	149.050	149.060	150.150	149.020	149.050	150.420
f	3.802	3.805	3.804	3.803	3.802	3.804

**Algorithm 1**

The pseudocode of the ASO.

---

**Input:** The population size N and maximum number of iterations T

**Output:** Optimal solutions and the location of skiers

Initialize the skiers population  $X_i (i = 1, 2, \dots, n)$ ;

Initialize step vectors  $\Delta X_i (i = 1, 2, \dots, n)$ ;

while stopping criteria is not satisfied do

  for each skier in population do

    the distance between each skier and the first place using Eq. (1)

    Calculate the physical stamina of each skier using Eq. (2)

  end for

  Find the first place of the skier:

  if no skier fall down neighbouring anyone skier

    Update velocity vector using Eq. (3)

    Update the position of the skiers using Eq. (4)

  else

    Update the position of the skiers using Eq. (5)

  else if

    Check and correct the new positions based on the boundaries of variables:

  end

  end while

---

**Acknowledgments**

This research work was supported by the National Natural Science Foundation of China (No. 52005081), Nonlinear equipment dynamics team of Henan Polytechnic University (T2019-5), Science and Technology Plan Project of Henan Province (No. 212102210226, No. 222102210182, No. 212102210004), Natural Science Foundation of Henan Polytechnic University (B2021-31), Henan Natural Science Foundation (No. 222300420168), Fundamental Research Funds for the Universities of Henan Province (NSFRF220415), Scientific Studies of Higher Education Institution of Henan province(22A520029), and the Key Discipline of Mechanical Engineering in Henan Polytechnic University.

**References**

- [1] Yuan Y, Lv L, Wang X, Song X. Optimization of a frame structure using the Coulomb force search strategy-based dragonfly algorithm. Eng Optim 2020;52(6): 915–31.
- [2] Yuan Y, Wang S, Lv L, Song X. An adaptive resistance and stamina strategy-based dragonfly algorithm for solving engineering optimization problems. Eng Comput 2021;38(5):2228–51.
- [3] Heidari AA, Mirjalili S, Faris H, Aljarah I, Mafarja M, Chen H. Harris hawks optimization algorithm and applications. Future Gener Comput Syst 2019;97: 849–72.
- [4] Vivek KP, Vimal JS. Heat transfer search (HTS): a novel optimization algorithm. Inform Sci 2015;324:217–46.
- [5] Yuan Y, Guo Z, Wang P, Song X. Multi-objective optimization of bucket wheel reclaimer based on improved dragonfly algorithm. Jixie Gongcheng Xuebao/J Mech Eng 2021;57(6):211–23.
- [6] Holland JH. Genetic algorithms. Sci Am 1992;267:66–73.
- [7] Karaboga D, Basturk B. A powerful and efficient algorithm for numerical function optimization: artificial bee colony (ABC) algorithm. J Glob Optim 2007;39:459–71.
- [8] Eberhart R, Kennedy J. A new optimizer using particle swarm theory. In: Proceedings of the sixth international symposium on micro machine and human science, MHS'95. IEEE; 1995. p. 39–43.
- [9] Storn R, Price K. Differential evolution-a simple and efficient heuristic for global optimization over continuous spaces. J Glob Optim 1997;11:34–359.
- [10] Gandomi AH, Yang X-S, Alavi AH. Cuckoo search algorithm: a metaheuristic approach to solve structural optimization problems. Eng Comput 2013;29:17–35.
- [11] Rashedi E, Nezamabadi-Pour H, Saryazdi S. GSA: a gravitational search algorithm. Inf Sci 2009;179:2232–48.
- [12] Dorigo M, Maniezzo V, Colorni A. Ant system: optimization by a colony of cooperating agents. IEEE Trans Syst Man Cybern B 1996;26:29–41.
- [13] Formato RA. Central force optimization. Prog Electromagn Res 2007;77:425–91.
- [14] Rao RV, Savsani VJ, Vakharia D. Teaching-learning-based optimization: an optimization method for continuous non-linear large scale problems. Inf Sci 2012; 183:1–15.
- [15] Hein D, Hentschel A, Runkler T, Udluft S. Particle swarm optimization for generating interpretable fuzzy reinforcement learning policies. Eng Appl Artif Intell 2017;65:87–98.
- [16] Zapata H, Perozo N, Angulo W, Contreras J. A hybrid swarm algorithm for collective construction of 3d structures. Int J Artif Intell 2020;18(1):1–18.
- [17] Precup RE, Hedrea EL, Roman RC, Petriu EM, Szedlak-Stinean A, Bojan-Dragos C. Experiment-based approach to teach optimization techniques. IEEE Trans Educ 2020;99:1–7.
- [18] Hein D, Hentschel A, Runkler T, Udluft S. Reinforcement learning with particle swarm optimization policy (pso-p) in continuous state and action spaces. Int J Swarm Intell Res 2016;7(3):23–42.
- [19] Roman R, Precup RE, Dragos CA, Szedlak-Stinean A. Combined Model-free adaptive control with fuzzy component by virtual reference feedback tuning for tower crane systems. Proced Comput Sci 2019;162:267–74.
- [20] Precup RE, David R, Roman RC, Petriu EM, Szedlak-Stinean A. Slime mould algorithm-based tuning of cost-effective fuzzy controllers for servo systems. Int J Comput Int Sys 2021;14(1):1042–52.
- [21] Yuan Y, Ren J, Zu J, Mu X. An adaptive instinctive reaction strategy based on Harris hawks optimization algorithm for numerical optimization problems. AIP Adv 2021;11(2):25012.
- [22] Wang G, Yuan Y, Guo W. An improved rider optimization algorithm for solving engineering optimization problems. IEEE Access 2019;7:80570–6.
- [23] Faramarzi A, Heidarinejad M, Stephens B, et al. Equilibrium optimizer: a novel optimization algorithm. Knowl Based Syst 2020;(191):105190.
- [24] Li S, Chen H, Wang M, et al. Slime mould algorithm: a new method for stochastic optimization. Future Gener Comp Syst 2020;(11):300–23.
- [25] Yuan YY, Mu XK, Shao XY, et al. Optimization of an auto drum fashioned brake using the elite opposition-based learning and chaotic k-best gravitational search strategy based grey wolf optimizer algorithm. Appl Soft Comput 2022;(123): 108947.
- [26] Premku Ma RM, Pradeep J, Sowmya R, et al. Multi-objective equilibrium optimizer: framework and development for solving multi-objective optimization problems. J Comput Des Eng 2021;(1):24–50.
- [27] Ahmed S, Sheikh KH, Mirjalili S, et al. Binary Simulated Normal Distribution Optimizer for feature selection: theory and application in COVID-19 datasets. Expert Syst Appl 2022;(200):116834.
- [28] Zhao W, Wang LY, Mirjalili S. Artificial hummingbird algorithm: a new bio-inspired optimizer with its engineering applications. Comput Method Appl Mech Eng 2022;(388):114194.
- [29] Dehkordi AA, Sadiq AS, Mirjalili S, et al. Nonlinear-based chaotic harris hawks optimizer: algorithm and internet of vehicles application. Appl Soft Comput 2021; 109:107574.
- [30] Askarzadeh A. Bird mating optimizer: an optimization algorithm inspired by bird mating strategies. Commun Nonlinear Sci Numer Simul 2014;19:1213–28.
- [31] Salcedo-Sanz S. Modern meta-heuristics based on nonlinear physics processes: a review of models and design procedures. Phys Rep 2016;655:1–70.
- [32] Wolpert DH, Macready WG. No free lunch theorems for optimization. IEEE Trans Evol Comput 1997;1:67–82.
- [33] Yu K, Wang X, Wang ZL. Multiple learning particle swarm optimization with space transformation perturbation and its application in ethylene cracking furnace optimization. Knowl Based Syst 2016;96(15):156–70.
- [34] Akira S, Aya T, Ryosuke A, Kohei W, Hiroshi A. Similarity of muscle synergies extracted from the lower limb including the deep muscles between level and uphill treadmill walking. Gait Posture 2018;59:134–9.
- [35] Yang XS. Nature-inspired metaheuristic algorithms. 2nd ed. Luniver Press; 2010.
- [36] Li ZM, Zhou YQ, Zhang S, Song JM. Lévy-flight moth-flame algorithm for function optimization and engineering design problems. Math Probl Eng 2016;8:1–22.
- [37] Aljarah I, Faris H, Mirjalili S. Lévy flight artificial bee colony algorithm. Int J Syst Sci 2016;47(9–12):2652–70.
- [38] More R, Lalit CS, Nilul S. Automatic generation control of a multi-area system using ant lion optimizer algorithm based PID plus second order derivative controller. Int J Electr Power Energy Syst 2016;80:52–63.

- [39] Satapathy SC, Naik A. Modified teaching-learning-based optimization algorithm for global numerical optimization-a comparative study. *Swarm Evol Comput* 2014; 16:28–37.
- [40] Seyedali M. The ant lion optimizer. *Adv Eng Softw* 2015;83:80–98.
- [41] Seyedali M. Moth-flame optimization algorithm: a novel nature-inspired heuristic paradigm. *Knowl Based Syst* 2015;89:228–49.
- [42] Qin AK, Huang VL, Suganthan PN. Differential evolution algorithm with strategy adaptation for global numerical optimization. *IEEE Trans Evol Comput* 2009;13(2): 398–417.
- [43] Nikolaus H, Sibylle DM, Petros K. Reducing the time complexity of the derandomized evolution strategy with covariance matrix adaptation (CMA-ES). *Evol Comput* 2003;11(1):1–18.
- [44] Seyedali M. Dragonfly algorithm: a new meta-heuristic optimization technique for solving single-objective, discrete, and multi-objective problems. *Neural Comput Appl* 2016;27(4):79–95.
- [45] Song J, Li S. Elite opposition learning and exponential function steps-based dragonfly algorithm for global optimization. Macau, China: Institute of Electrical and Electronics Engineers Inc.; 2017. p. 1178–83.
- [46] Saremi S, Mirjalili S, Lewis A. Grasshopper optimisation algorithm: theory and application. *Adv Eng Softw* 2017;105:30–47.
- [47] Gandomi AH, Yang XS, Alavi AH. Cuckoo search algorithm: a metaheuristic approach to solve structural optimization problems. *Eng Comput* 2013;29:17–35.
- [48] Tsai JF. Global optimization of nonlinear fractional programming problems in engineering design. *Eng Optim* 2005;37:399–409.
- [49] Ray T, Saini P. Engineering design optimization using a swarm with an intelligent information sharing among individuals. *Eng Optim* 2001;33:735–48.
- [50] Liu H, Cai Z, Wang Y. Hybridizing particle swarm optimization with differential evolution for constrained numerical and engineering optimization. *Appl Soft Comput* 2010;10:629–40.
- [51] Zhao WG, Wang LY, Mirjalili S. Artificial hummingbird algorithm: a new bio-inspired optimizer with its engineering applications. *Comput Methods Appl Mech Eng* 2022;388:114194.
- [52] Eskandar H, Sadollah A, Bahreininejad A, Hamdi M. Water cycle algorithm-a novel metaheuristic optimization method for solving constrained engineering optimization problems. *Comput Struct* 2012;110:151–66.
- [53] Rao RV, Savsani VJ, Vakharia D. Teaching-learning-based optimization: a novel method for constrained mechanical design optimization problems. *Comput Aided Des* 2011;43:303–15.
- [54] Savsani P, Savsani V. Passing vehicle search (pvs): a novel metaheuristic algorithm. *Appl Math Model* 2016;40:3951–78.
- [55] Rao BR, Tiwari R. Optimum design of rolling element bearings using genetic algorithms. *Mech Mach Theory* 2007;42(2):233–50.
- [56] Wang Y, Cai Z, Zhou Y, Fan Z. Constrained optimization based on hybrid evolutionary algorithm and adaptive constraint-handling technique. *Struct Multidiscip Optim* 2009;37(4):395–413.
- [57] Liu H, Cai Z, Wang Y. Hybridizing particle swarm optimization with differential evolution for constrained numerical and engineering optimization. *Appl Soft Comput* 2010;10(2):629–40.
- [58] Wang L, Li L. An effective differential evolution with level comparison for constrained engineering design. *Struct Multidiscip Optim* 2010;41(6):947–63.
- [59] de Melo VV, Carosio GL. Investigating multi-view differential evolution for solving constrained engineering design problems. *Expert Syst Appl* 2013;40(9):3370–7.
- [60] Gupta S, Tiwari R, Nair SB. Multi-objective design optimisation of rolling bearings using genetic algorithms. *Mech Mach Theory* 2007;42:1418–43.
- [61] Zhao W, Zhang Z, Wang L. Manta ray foraging optimization: an effective bio-inspired optimizer for engineering applications. *Eng Appl Artif Intell* 2020;87(1): 103300.